



Published in final edited form as:

J Am Soc Mass Spectrom. 2021 July 07; 32(7): 1631–1637. doi:10.1021/jasms.1c00091.

Simultaneous evaluation of a vaccine component micro-heterogeneity and conformational integrity using native mass spectrometry and limited charge reduction

Cedric E. Bobst¹, Justin Sperry², Olga V. Friese², Igor A. Kaltashov^{1,*}

¹Department of Chemistry, University of Massachusetts-Amherst, Amherst, MA 01003;

²BioTherapeutics Pharmaceutical Sciences, Pfizer, St. Louis, MO 63017

Abstract

Analytical characterization of extensively modified proteins (such as haptenated carrier proteins in synthetic vaccines) remains a challenging task due to the high degree of structural heterogeneity. Native mass spectrometry (MS) combined with limited charge reduction allows these obstacles to be overcome and enables meaningful characterization of a heavily haptenated carrier protein CRM197 (inactivated diphtheria toxin conjugated with nicotine), a major component of a smoking cessation vaccine. The extensive conjugation results in a near-continuum distribution of ionic signal in electrospray ionization (ESI) mass spectra of haptenated CRM197 even after size-exclusion chromatographic fractionation. However, supplementing the ESI MS measurements with limited charge reduction of ionic populations selected within narrow m/z windows gives rise to well-resolved charge ladders, from which both masses and charge states of the ionic species can be readily deduced. Application of this technique to a research-grade material of CRM197/H7 conjugate not only reveals its marginal conformational stability (manifested by the appearance of high charge-density ions in ESI MS), but also establishes a role of the extent of haptenation as a major factor driving the loss of the higher order structure integrity. The unique information provided by native MS used in combination with limited charge reduction provides a strong argument for this technique to become a standard/required tool in the analytical arsenal in the field of biotechnology and biopharmaceutical analysis, where protein conjugates are becoming increasingly common.

Graphical Abstract

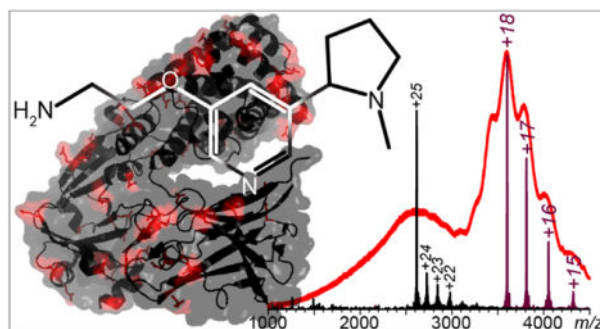
* Address correspondence to: Igor A. Kaltashov, kaltashov@chem.umass.edu.

Author Contributions

J.S., O.F and I.K designed the study, C.B. and I.K. designed the experimental work, C.B. carried out the experimental work, C.B. and I.K. interpreted the data, I.K. wrote the manuscript. All authors gave their consent to the final (submitted) version of the manuscript.

Supporting Information

Supplementary Information contains the results of MaxEnt and UniDec deconvolution of the ESI MS data presented in Figure 3, and is available free of charge on the ACS Publications website.



Introduction

In the past decade mass spectrometry (MS) has become a major tool in the analytical arsenal used for characterization of a range of biopharmaceutical products, particularly recombinant proteins-based therapeutics.^{1–3} However, the ever-increasing complexity and sophistication of modern biopharmaceuticals continues to present novel challenges vis-à-vis analytical work. Modern vaccines are one example of exceedingly sophisticated biotechnological products whose characterization requires that novel analytical approaches be developed to meet and address these challenges. While the COVID-19 pandemic understandably put in the spotlight vaccines that employ either viral particles⁴ or liposomes⁵ as delivery vectors, a wide range of modern vaccines utilize extensive haptentation⁶ of carrier proteins (such as the enzymatically inactive and non-toxic mutant of the diphtheria toxin CRM197⁷), presenting formidable challenges vis-à-vis analytical characterization. Haptents are low molecular weight molecules that must be conjugated to proteins in order to enable their recognition by the immune system,⁶ allowing vaccines to be developed against targets that are too small to be immunogenic on their own (*e.g.*, nicotine, methamphetamine, opioids, *etc.*).

Common issues with the nicotine vaccines in the past were relatively low and variable antibody levels,⁸ prompting extensive efforts to correlate structural characteristics of the conjugates with the immune response.^{9–11} While both the choice of a specific haptent and the conjugation chemistry, as well as the haptent load are known to influence the extent of the immune response, tertiary structure of the carrier protein was also recently shown to play a role (with the conjugates that have more open structure eliciting lower functional response).¹¹ More extensive chemical modification is likely to favor open conformations of the carrier protein, suggesting that there is an optimal extent of haptentation that generates best immune response upon vaccination. Clearly, there is a need for analytical techniques that allow both the covalent structure of the vaccine components (the haptent load) and the integrity of the higher order structure to be evaluated simultaneously in a fast yet reliable fashion to provide valuable information during both the design and production stages. While native MS has proven to be a powerful technique to correlate structural changes within protein pharmaceuticals (such as non-enzymatic post-translational modifications) with the integrity of the higher order structure,^{12,13} this task is made challenging in the case of synthetic vaccine components due to their extreme levels of structural heterogeneity.

In recent years a range of experimental approaches had been developed aiming at extracting meaningful information from the MS measurements of macromolecular systems exhibiting high levels of structural heterogeneity, and supplementing MS measurements with gas-phase ion-molecular and ion-ion reactions proved particularly useful in this regard.^{14,15} Specifically, a technique based on limited charge reduction of macromolecular ions in the gas phase¹⁶ has been particularly effective as a means of characterizing highly heterogeneous systems ranging from PEGylated proteins¹⁷ to unfractionated heparin.¹⁸ In this work we explore the utility of this technique as a means of evaluating both the extent of haptation and the conformational integrity of CRM197 conjugated with a nicotine-mimicking hapten H7.⁹

Experimental

Materials.

The CRM197/H7 conjugate was produced using a one-pot four-component reaction (a single-point non-toxic mutant of diphtheria toxin CRM197; nicotine analogue H7; a zero-length cross-linker EDC, 1-ethyl-3-(3-dimethylaminopropyl)carbodiimide hydrochloride; and a bi-functional cross-linker sNHS, sulfo-N-hydroxysuccinimide) as described elsewhere.^{10,11} All solvents and buffers used in this work were of analytical grade or higher. All protein solutions for MS analysis were prepared at pH 5.5 to ensure maximum stability of the CRM197/H7 conjugate.

Methods.

Size-exclusion chromatographic separations were carried out using two TSKGel G3000swxl (Tosoh, Tokyo, Japan) columns connected in series with an HP1100 (Agilent Technologies, Santa Clara, CA) liquid chromatograph. A 100 mM aqueous ammonium acetate solution was used as a mobile phase (pH adjusted to 5.5); absorption at 280 nm was used for detection. MALDI MS measurements were carried out in a positive-ion, linear mode using ultrafleXtreme™ (Bruker Daltonics, Billerica, MA) MALDI time-of-flight mass spectrometer. ESI MS measurements were carried out using a Synapt G2Si (Waters, Milford, MA) hybrid quadrupole/time-of-flight mass spectrometer equipped with a standard nanospray source and a glow discharge source for introducing 1,3-dicyanobenzene radical anions. All samples were analyzed in the nanospray mode using pre-fabricated emitters ES380 (ThermoFisher Scientific, Waltham, MA). A capillary voltage of 1,000 V was used for all measurements. The dry gas was set to a flow of 300 L/hr and a temperature of 150 °C. Limited charge reduction measurements were carried out using electron transfer dissociation (ETD) by isolating precursor ions using the front-end quadrupole followed by their exposure to a charge-transfer reagent (1,3-dicyanobenzene radical anions) in the trap cell. The following ETD parameters were used: the glow discharge current of 80 μ A, the makeup gas flow of 25 mL/min. The ETD reagent refill time was 0.1 s, and the trap cell T-wave used a height of 0.25 V and velocity of 250 m/s.

Results and Discussion

Conjugation of CRM197 with the nicotine analog H7 targets side chains of acidic amino acid residues, and each conjugation event is expected to result in a mass increase of ca. 203 Da (see Scheme 1). While the total number of carboxylic groups within the protein is sixty-six (twenty-eight aspartic acid residues, thirty-seven glutamic acid residues and the C-terminal α -carboxylate), the hapten density assay (removing H7 from the conjugate by acid hydrolysis followed by H7 quantitation using HPLC) indicated that on average 11–13 haptens are conjugated to the carrier protein. The expected mass increase for this level of hapten density is 2.2–2.6 kDa; however, the MALDI MS analysis of the CRM197/H7 conjugate reveals a mass increase that is almost twice as high, with the mass distribution spanning a 5-kDa region (Figure 1). This discrepancy is not surprising, given the fact that the cross-linking chemistry used to produce the CRM197/H7 conjugate is likely to generate multiple byproducts, such as EDC/tyrosine covalent adducts. Furthermore, MALDI-generated ions are known to be prone to non-covalent adduct formation, which would result in overestimation of the extent of chemical modification of the carrier protein (an opposite effect would be produced by in-source fragmentation, which may increase ionic intensity at the lower end of the mass distribution). Lastly, MALDI MS provides no indication vis-à-vis compactness/conformational integrity of the haptenated carrier protein.

In order to evaluate the influence of the chemical modification on the higher order structure integrity of the CRM197/H7 conjugate, both unmodified and haptenated forms of the carrier protein were analyzed with size exclusion chromatography (SEC). Not surprisingly, the unmodified protein eluted as a single peak (elution window 19.0–19.5 min, consistent with the monomeric structure of the protein), with a low-abundance earlier-eluting species (17.5 min) indicating the presence of a small amount of soluble high-molecular weight aggregates (Figure 2). In contrast, the elution profile of haptenated CRM197 is very convoluted and consists of two broad partially overlapping peaks, one confined to the 19.5–21.0 min elution window, and another one spanning a 17.0–19.5 min window (with significant front-end tailing apparent at elution time as early as 15 min). The delayed elution of a large fraction of the CRM197/H7 conjugate (elution window 19.5–21.0 min) compared to the unmodified protein may seem surprising, as the extensive chemical modification is not expected to cause the protein adopt a more compact conformation. However, the physical size of a macromolecule is not the sole determinant of its elution time in SEC, as the electrostatic interactions may also play a role. Indeed, the significant decrease of the protein pI as a result of the chemical modification of a large number of acidic side chains in the course of haptenation is likely to reduce the repulsion between the protein and the partially deprotonated silica surface of the SEC column packing material, thereby causing the elution time increase. At the same time, the presence of an abundant early-elution peak in the CRM197/H7 chromatogram clearly indicates significant conformational heterogeneity within the haptenated protein sample, although it remains unclear whether these early-eluting species represent soluble aggregates or partially unfolded monomeric species.

In order to characterize both the mass distribution and the extent of conformational heterogeneity of CRM197/H7, the two major SEC fractions (fractions 9 and 12 in Figure

2) were collected and characterized off-line using electrospray ionization (ESI) MS, and compared to the intact (unmodified) CRM197. Consistent with the MALDI MS data, the ESI mass spectrum of the intact CRM197 is indicative of a homogeneous protein with the mass being consistent with the CRM197 polypeptide sequence (see the black trace in Figure 3). Furthermore, the narrow distribution of the charge states (+15 through +18) in this mass spectrum is consistent with the notion of the intact protein maintaining compact conformation in solution. In contrast, the mass spectra of the two fractions of the haptenated protein provide evidence of a significant mass increase as a result of conjugation. Importantly, the mass increase appears to be notably higher within the earlier-eluting species (compare the red and blue traces in Figure 3). Furthermore, the ionic signal in the mass spectrum of fraction 9 is distributed over a significantly wider m/z range. Although this spectral feature can be interpreted as a result of the protein unfolding in solution giving rise to high charge-density ions (populating m/z region 1,500–3,000), the poor spectral resolution does not allow the charge state assignment to be made and the masses to be determined. In fact, the significant extent of structural heterogeneity is also responsible for the broad and poorly-defined ionic peaks in the higher m/z region of the mass spectrum (3,000–4,500), making the charge state/mass assignment a challenging task for this part of the ionic population as well. Likewise, even though the extent of structural heterogeneity exhibited by CRM197/H7 fraction 12 appears to be somewhat lower compared to fraction 9, it is nonetheless sufficiently high to generate broad, partially overlapping peaks in the mass spectrum (the blue trace in Figure 3), a feature that can produce an error in assigning the ionic charge states.^{16,19} Indeed, our initial attempts to interpret this spectrum using the MaxEnt-based deconvolution routine integrated into the data analysis software resulted in a mass distribution that was clearly inconsistent with the MALDI MS data (a series of peaks spaced by ca. 4 kDa and populating a 40,000–70,000 Da mass range, see Supplementary Material for more detail). Similarly disappointing results were obtained with the publicly available UniDec deconvolution algorithm²⁰ (see Supplementary Material for more detail).

Meaningful interpretation of the ESI MS data was enabled by applying limited charge reduction, a technique that uses charge-transfer reactions in the gas phase to generate well-defined charge ladders for ionic species selected within relatively narrow m/z windows.¹⁶ An example of using this technique for the analysis of CRM197/H7 fraction 12 is presented in Figure 4, where selection of two narrow populations of precursor ions close to the apex of the ionic peak in the original ESI mass spectrum generates well-resolved ladders, from which both the charge states and the masses of the precursor ions can be readily determined. Sampling the precursor ion populations for subsequent limited charge reduction measurements across a wide range of ionic species present in the original mass spectrum allows the mass of the most abundant species to be determined as 63.2 kDa, with the distribution spanning the range over 1 kDa (see the diagram in Figure 4B). One interesting feature of the mass spectra of the limited charge reduction products is the presence of ions whose masses are consistent with putative adducts formed by non-covalent association of 1,3-dicyanobenzene with either the precursor ions or partially reduced ions (labeled with triangles in Figure 4A). While the presence of such ions in the mass spectra is not surprising (given the fact that the charge-transfer process likely involves formation of a transient polycation/radical anion complex), such species have not been reported previously, and the

possibility of their existence should certainly be taken into consideration when the results of limited charge reduction measurements are analyzed.

Another peculiar feature of the ESI mass spectrum of CRM197/H7 fraction 12 shown in Figure 3 that is notably absent in the reference mass spectrum of the intact CRM is the presence of low-abundance, but nonetheless readily identifiable higher charge states at m/z below 3,300 (corresponding to charge states +20 through +25). The presence of higher charge-density ionic species in ESI MS alongside a narrow distribution of low charge-density ions usually reflects partial protein unfolding in solution.²¹ The low relative abundance of these ions indicate that the Boltzmann weight of the less compact protein species is low (most likely a result of transient unfolding). The high-charge density ionic signal ($m/z < 3,300$) is significantly more pronounced in the ESI mass spectrum of CRM197/H7 fraction 9 (Figure 5). Limited charge reduction measurements provide a mass value for the most abundant ions in this m/z range as 65.4 kDa, which only slightly exceeds the masses of ionic populations near the apex of the most abundant low charge-density peak (precursor ion m/z values 3590, 3600, and 3610) which fall within the 64.6–64.9 kDa range (low-abundance ionic species with masses as high as 68.4 kDa have also been detected). It is noteworthy that the mass of the conjugate in fraction 9 is considerably higher compared to that of fraction 12 (by *ca.* 1.5 kDa), and the higher extent of chemical modification clearly correlates with the decreased conformational stability.

The relationship between the conformation of the protein carrier and the extent of its conjugation/chemical modification was previously noted for CRM197/peptide conjugates.²² This correlation was hypothesized to originate from alkylation of a specific residue (histidine 21), which induces a non-native (open) conformation of the protein, thereby enabling reagents' access to the side chains that are inaccessible in the native (closed) conformation.²² The ensuing ligation of these sites with the peptide haptens further stabilizes the open conformation. The two SEC chromatographic peaks observed in that study had similar characteristics to CRM197/H7 fractions 9 and 12 reported in our work (see Figure 2), and were interpreted as a result of two distinct conformations separated chromatographically based on the difference in their physical size (hydrodynamic radius) in solution. Supplementing SEC measurements with native ESI MS and limited charge reduction argues for a more nuanced picture, with both moderately and extensively modified forms of the carrier protein (fractions 12 and 9, respectively) capable of sampling both native-like compact and more extended (open) conformations, rather than each being locked in a single conformation reflecting the specific extent of haptentation. The presence of the high charge-density ions in ESI mass spectra of both forms of the protein (albeit with dramatically different levels of relative abundance) suggest that the difference between them is quantitative, rather than qualitative. Indeed, low abundance of the ionic signal at charge states exceeding $z = +19$ in the mass spectrum of CRM197/H7 fraction 12 (the blue trace in Figure 3) indicates that the less compact (open) conformation is sampled transiently, and the integrity of the higher order structure is mostly maintained. The dramatic increase of the Boltzmann weight of the open conformation triggered by more extensive modification of the carrier protein manifests itself by a notable elevation of the relative abundance of the high charge-density ionic signal, which is evident in the mass spectrum of CRM197/H7 fraction 9 (the red trace in Figure 3). In both cases the equilibrium between the two conformations

is fast on the chromatographic time scale, and the distinct elution windows of the two forms of the protein reflect the influence exerted by the extent of haptentation on the equilibrium between the closed (native-like) and open (partially disordered) conformations.

Analysis of protein ion charge state distributions in native MS has become a commonly accepted tool in the analysis of conformational integrity of therapeutic proteins,²³ although its application to other biopharmaceutical products (especially those exhibiting high degrees of structural heterogeneity, such as haptentated carrier proteins) remain limited. Supplementing ESI MS measurements with limited charge reduction in the gas phase not only provides an elegant way towards evaluating the extent of CRM197 haptentation, but also allows the emergence of bimodal charge state distribution in the ESI mass spectra to be observed, thereby enabling detection of conformational transitions within the carrier protein that have been previously demonstrated to be important attenuators of the vaccine's functional response. This unique information cannot be extracted from either MS or SEC measurements alone, highlighting the value of this new approach in the field of vaccine characterization. While the focus of this pilot study was a smoking cessation vaccine that utilizes a nicotine analog as a hapten, it is important to note that smoking addiction and substance abuse are not the only pathologies targeted by the so-called "synthetic vaccine" approach based on conjugation of small antigens to a carrier protein.²⁴ In fact, one of the anti-SARS-CoV-2 vaccines currently undergoing Phase III clinical trials, EpiVacCorona²⁵ uses peptide antigens (short segments of SARS-CoV-2 spike protein) as haptens conjugated to a carrier protein,²⁶ and other antiviral vaccines utilizing similar design strategies are likely to follow. The means of their analytical characterization are currently limited, and the approach evaluated in this work will undoubtedly provide a wealth of information on the structural features of these vaccines' components that are important determinants of their efficacy and safety.

Conclusions

Charge state distributions in native ESI MS provide important information on protein higher order structure, but the applications using this feature in the field of biopharmaceutical analysis had been limited to relatively homogeneous systems, such as minimally modified recombinant proteins. The high levels of structural heterogeneity frequently encountered in many biopharmaceutical products make ESI MS analyses challenging, as the wide distributions of macromolecular masses give rise to overlapping ion peaks in the ESI mass spectra, and in some extreme cases can lead to near-continuum distributions of the ionic signal. Complementing ESI MS measurements with limited charge reduction in the gas phase allows meaningful mass information to be extracted from such poorly- or completely un-resolved mass spectra, yielding both ionic mass and charge values. The latter can be used as a means of evaluating the integrity of the macromolecular higher order structure, and in the case of haptentated carrier proteins allows the correlations between the extent of protein modification and its conformational stability to be established. Application of this technique to CRM197/H7, an active component of a smoking cessation vaccine, allows two distinct forms of the conjugate to be characterized and provides a more nuanced view of the relationship between the extent of conjugation/modification of the carrier protein and its conformation. In contrast to the previous models that postulate the existence of two

distinct conformations for the moderately and extensively haptenated carrier protein, our analysis suggests that each form of the protein continuously samples both native (closed) and partially disordered (open) conformations in solution, although their Boltzmann weights show strong dependence on the extent of protein modification. The unique information provided by this approach makes a strong argument supporting the view that native MS complemented with limited charge reduction and SEC should become de rigueur in the intact-mass analysis of biopharmaceutical products exhibiting extreme levels of structural heterogeneity, including targets as challenging as components of synthetic vaccines.

Supplementary Material

Refer to Web version on PubMed Central for supplementary material.

ACKNOWLEDGMENT

This work was supported in part by the grants from the National Science Foundation (CHE-1709552) and the National Institutes of Health (R01 GM132673). The FT ICR mass spectrometer was acquired through the grant CHE-0923329 from the National Science Foundation (Major Research Instrumentation program) and is now operated by the UMass-Amherst Mass Spectrometry Facility.

REFERENCES

- (1). Carini M; Regazzoni L; Aldini G Mass Spectrometric Strategies and Their Applications for Molecular Mass Determination of Recombinant Therapeutic Proteins. *Curr. Pharm. Biotechnol* 2011, 12, 1548–1557. [PubMed: 21542798]
- (2). Kaltashov IA; Bobst CE; Abzalimov RR; Wang G; Baykal B; Wang S Advances and challenges in analytical characterization of biotechnology products: Mass spectrometry-based approaches to study properties and behavior of protein therapeutics. *Biotechnol. Adv* 2012, 30, 210–222. [PubMed: 21619926]
- (3). Zhang H; Cui W; Gross ML Mass spectrometry for the biophysical characterization of therapeutic monoclonal antibodies. *FEBS Lett.* 2014, 588, 308–317. [PubMed: 24291257]
- (4). Logunov DY; Dolzhikova IV; Zubkova OV; Tukhvatullin AI; Shcheblyakov DV; Dzharullaeva AS; Grousova DM; Erokhova AS; Kovyrshina AV; Botikov AG; Izhaeva FM; Popova O; Ozharovskaya TA; Esmagambetov IB; Favorskaya IA; Zrelkin DI; Voronina DV; Shcherbinin DN; Semikhin AS; Simakova YV, et al. Safety and immunogenicity of an rAd26 and rAd5 vector-based heterologous prime-boost COVID-19 vaccine in two formulations: two open, non-randomised phase 1/2 studies from Russia. *Lancet* 2020, 396, 887–897. [PubMed: 32896291]
- (5). Polack FP; Thomas SJ; Kitchin N; Absalon J; Gurtman A; Lockhart S; Pérez Marc G; Moreira ED; Zerbini C; Bailey R; Swanson KA; Roychoudhury S; Koury K; Li P; Kalina WV; Cooper D; Frenck RW Jr.; Hammitt LL; Türeci Ö, et al. Safety and Efficacy of the BNT162b2 mRNA Covid-19 Vaccine. *N. Engl. J. Med* 2020, 383, 2603–2615. [PubMed: 33301246]
- (6). Chipinda I; Hettick JM; Siegel PD Haptenation: Chemical Reactivity and Protein Binding. *J. Allergy* 2011, 2011, 839682.
- (7). Knuf M; Kowalzik F; Kieninger D Comparative effects of carrier proteins on vaccine-induced immune response. *Vaccine* 2011, 29, 4881–4890. [PubMed: 21549783]
- (8). Cornish KE; de Villiers SH; Pravetoni M; Pentel PR Immunogenicity of individual vaccine components in a bivalent nicotine vaccine differ according to vaccine formulation and administration conditions. *PloS one* 2013, 8, e82557. [PubMed: 24312662]
- (9). Pryde DC; Jones LH; Gervais DP; Stead DR; Blakemore DC; Selby MD; Brown AD; Coe JW; Badland M; Beal DM; Glen R; Wharton Y; Miller GJ; White P; Zhang N; Benoit M; Robertson K; Merson JR; Davis HL; McCluskie MJ Selection of a Novel Anti-Nicotine Vaccine: Influence of Antigen Design on Antibody Function in Mice. *PloS one* 2013, 8, e76557. [PubMed: 24098532]

- Author Manuscript
- Author Manuscript
- Author Manuscript
- Author Manuscript
- (10). McCluskie MJ; Thorn J; Mehelic PR; Kolhe P; Bhattacharya K; Finneman JJ; Stead DR; Piatchek MB; Zhang N; Chikh G; Cartier J; Evans DM; Merson JR; Davis HL Molecular attributes of conjugate antigen influence function of antibodies induced by anti-nicotine vaccine in mice and non-human primates. *Int. Immunopharmacol* 2015, 25, 518–527. [PubMed: 25737198]
 - (11). Thorn JM; Bhattacharya K; Crutcher R; Sperry J; Isele C; Kelly B; Yates L; Zobel J; Zhang N; Davis HL; McCluskie MJ The Effect of Physicochemical Modification on the Function of Antibodies Induced by Anti-Nicotine Vaccine in Mice. *Vaccines* 2017, 5, 11.
 - (12). Bobst CE; Abzalimov RR; Houde D; Kloczewiak M; Mhatre R; Berkowitz SA; Kaltashov IA Detection and characterization of altered conformations of protein pharmaceuticals using complementary mass spectrometry-based approaches. *Anal. Chem* 2008, 80, 7473–7481. [PubMed: 18729476]
 - (13). Bobst CE; Thomas JJ; Salinas P; Savickas P; Kaltashov IA Impact of oxidation on protein therapeutics: Conformational dynamics of intact and oxidized acid- β -glucocerebrosidase at near-physiological pH. *Protein Sci.* 2010, 19, 2366–2378. [PubMed: 20945356]
 - (14). Foreman DJ; McLuckey SA Recent Developments in Gas-Phase Ion/Ion Reactions for Analytical Mass Spectrometry. *Anal. Chem* 2020, 92, 252–266. [PubMed: 31693342]
 - (15). McLuckey SA; Goeringer DE Ion/Molecule Reactions for Improved Effective Mass Resolution in Electrospray Mass Spectrometry. *Anal. Chem* 1995, 67, 2493–2497. [PubMed: 8686879]
 - (16). Abzalimov RR; Kaltashov IA Electrospray ionization mass spectrometry of highly heterogeneous protein systems: Protein ion charge state assignment via incomplete charge reduction. *Anal. Chem* 2010, 82, 7523–7526. [PubMed: 20731408]
 - (17). Muneeruddin K; Bobst CE; Frenkel R; Houde D; Turyan I; Sosic Z; Kaltashov IA Characterization of a PEGylated protein therapeutic by ion exchange chromatography with on-line detection by native ESI MS and MS/MS. *Analyst* 2017, 142, 336–344. [PubMed: 27965993]
 - (18). Zhao Y; Abzalimov RR; Kaltashov IA Interactions of Intact Unfractionated Heparin with Its Client Proteins Can Be Probed Directly Using Native Electrospray Ionization Mass Spectrometry. *Anal. Chem* 2016, 88, 1711–1718. [PubMed: 26707758]
 - (19). Abzalimov RR; Bobst CE; Salinas PA; Savickas P; Thomas JJ; Kaltashov IA Studies of pH-dependent self-association of a recombinant form of arylsulfatase A with electrospray ionization mass spectrometry and size-exclusion chromatography. *Anal. Chem* 2013, 85, 1591–1596. [PubMed: 23252501]
 - (20). Marty MT; Baldwin AJ; Marklund EG; Hochberg GK; Benesch JL; Robinson CV Bayesian deconvolution of mass and ion mobility spectra: from binary interactions to polydisperse ensembles. *Anal. Chem* 2015, 87, 4370–4376. [PubMed: 25799115]
 - (21). Kaltashov IA; Abzalimov RR Do ionic charges in ESI MS provide useful information on macromolecular structure? *J. Am. Soc. Mass Spectrom* 2008, 19, 1239–1246. [PubMed: 18602274]
 - (22). Jaffe J; Wucherer K; Sperry J; Zou Q; Chang Q; Massa MA; Bhattacharya K; Kumar S; Caparon M; Stead D; Wright P; Dirksen A; Francis MB Effects of Conformational Changes in Peptide-CRM(197) Conjugate Vaccines. *Bioconjug. Chem* 2019, 30, 47–53. [PubMed: 30475601]
 - (23). Kaltashov IA; Bobst CE; Pawlowski J; Wang G Mass spectrometry-based methods in characterization of the higher order structure of protein therapeutics. *J. Pharm. Biomed. Anal* 2020, 184, 113169. [PubMed: 32092629]
 - (24). Jones LH Recent advances in the molecular design of synthetic vaccines. *Nat. Chem* 2015, 7, 952–960. [PubMed: 26587710]
 - (25). Onishchenko GG; Sizikova TE; Lebedev VN; S.V. B Analysis of Promising Approaches to COVID-19 Vaccine Development. *BIOPreparations. Prevention, Diagnosis, Treatment* 2020, 20, 216–227.
 - (26). Ryzhikov AB; Ryzhikov EA; Bogryantseva MP; Usova SV; Danilenko ED; Nechaeva EA; Pyankov OV; Pyankova OG; Gudymo AS; Bodnev SA; Onkhonova GS; Sleptsova ES; Kuzubov VI; Ryndyuk NN; Ginko ZI; Petrov VN; Moiseeva AA; Torzhkova PY; Pyankov SA; Tregubchak TV, et al. A single blind, placebo-controlled randomized study of the safety, reactogenicity and

immunogenicity of the “EpiVacCorona” vaccine for the prevention of COVID-19, in volunteers aged 18–60 years (phase I-II). *Infektsiya Immun.* 2021, 11, 283–296.

Author Manuscript

Author Manuscript

Author Manuscript

Author Manuscript

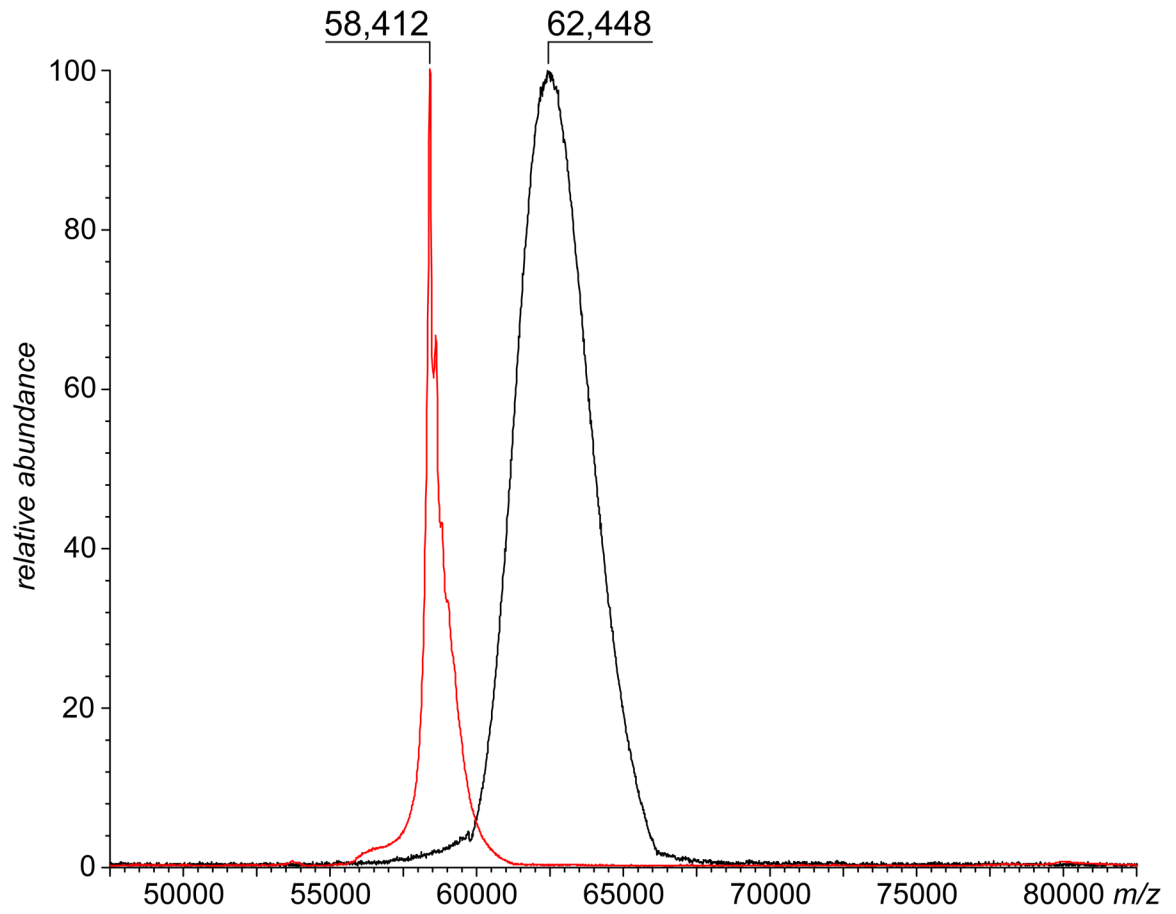


Figure 1. MALDI mass spectra of intact (unmodified) CRM197 and CRM197/H7 (red and black traces, respectively).

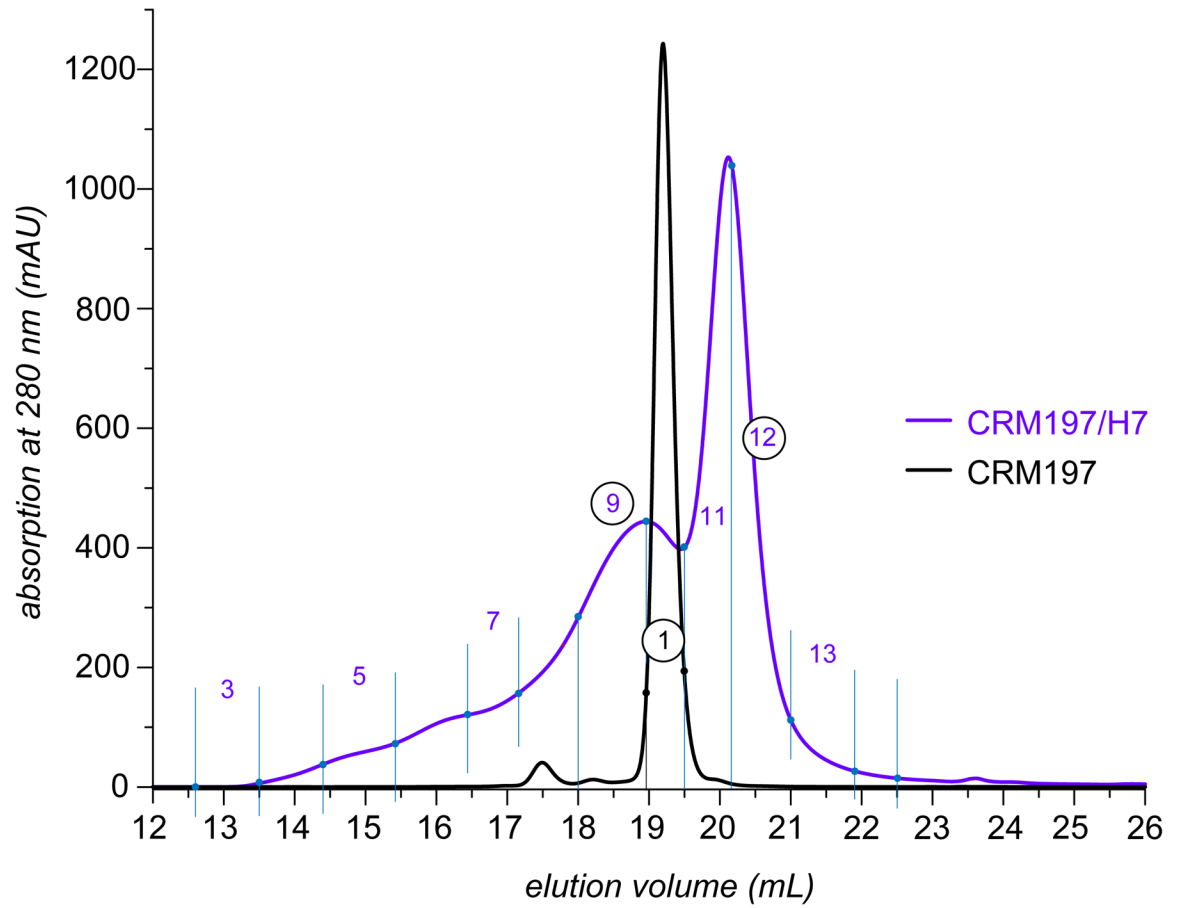


Figure 2. SEC UV-chromatograms of intact (unmodified) CRM197 and CRM197/H7 (black and blue traces, respectively).

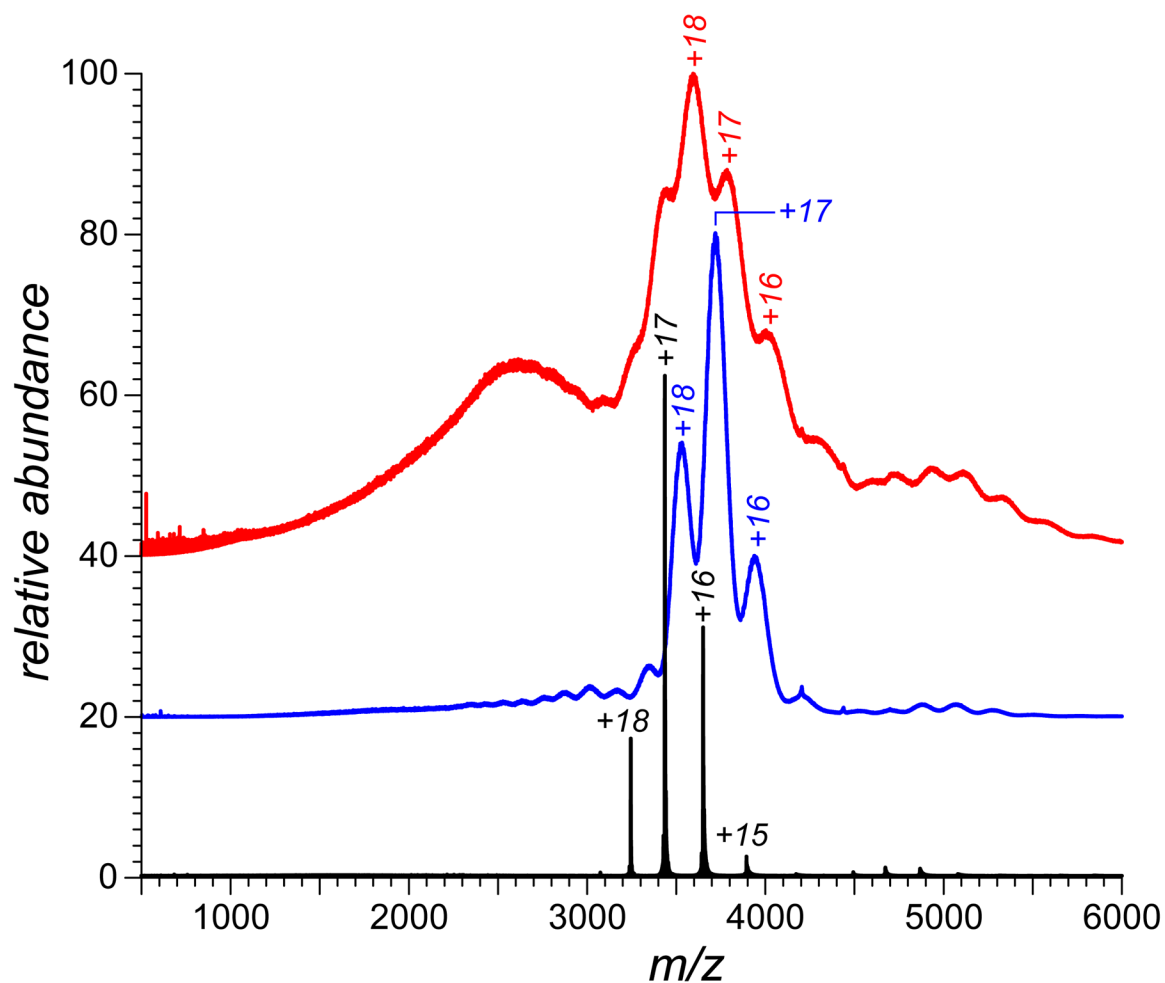


Figure 3. ESI MS analysis of two SEC fractions of CRM197/H7 (fraction 9, red trace; and fraction 12, blue trace). The black trace shows a reference mass spectrum of intact (unmodified) CRM197 (SEC fraction 1). The SEC fraction numbers refer to data presented in Figure 2.

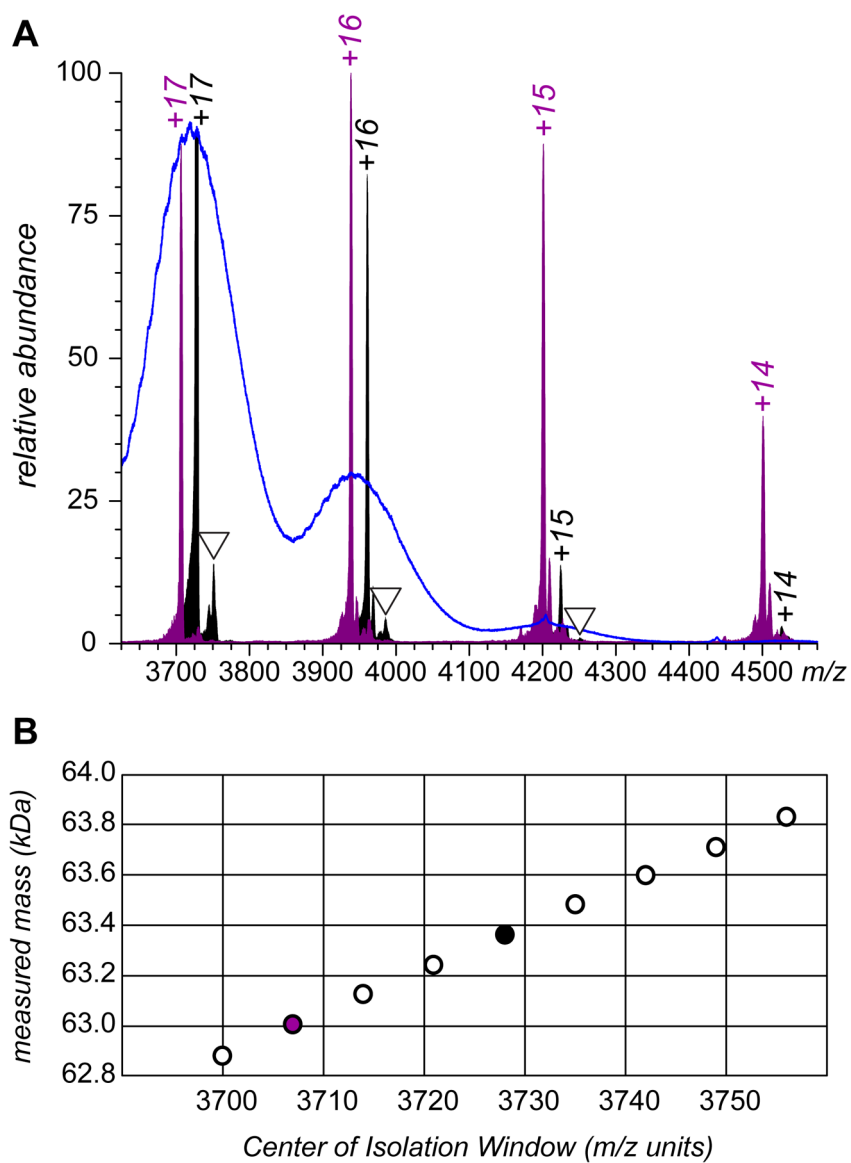


Figure 4. Limited charge reduction analysis of ESI-generated ionic species (CRM197/H7, SEC fraction 12) showing two representative charge ladders produced by inducing charge-transfer reactions in the gas phase (**A**) and calculated ionic masses for all precursor ions subjected to the charge-transfer reactions (**B**).

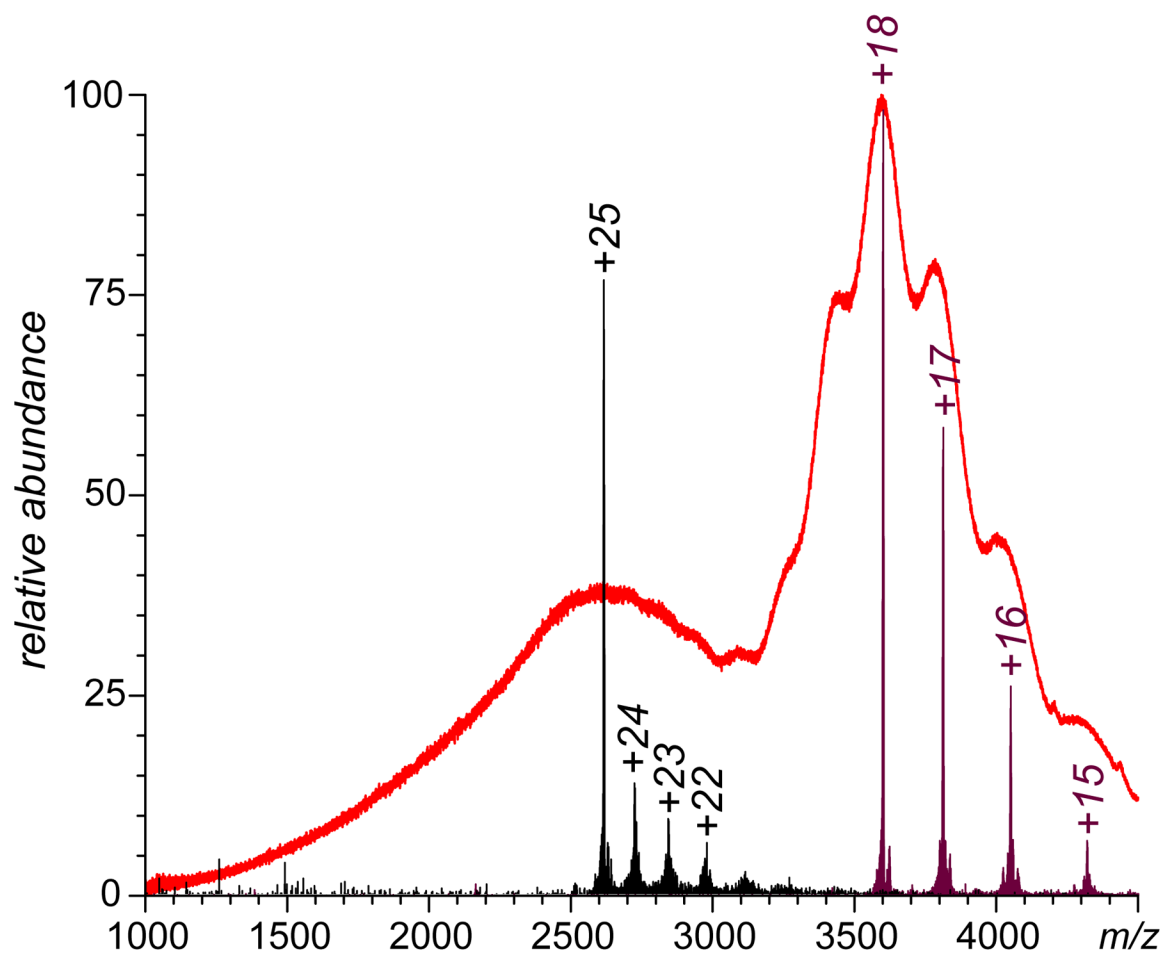
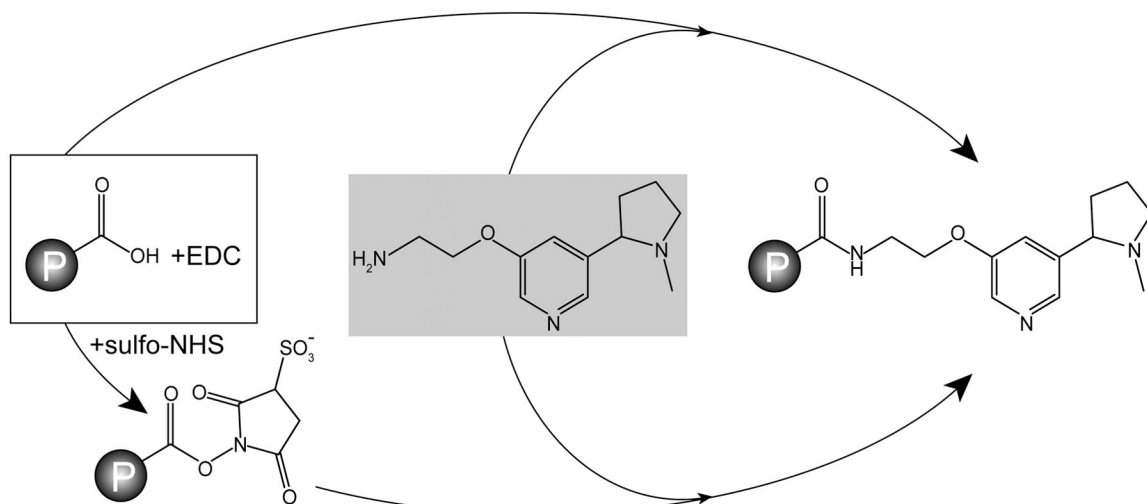


Figure 5. Limited charge reduction analysis of ESI-generated ionic species (CRM197/H7, SEC fraction 9) showing representative charge ladders produced by inducing charge-transfer reactions using high- and low-charge density polycations (the black and purple traces, respectively).

**Scheme 1.**

A schematic representation of the CRM197/H7 conjugate production using a one-pot four-component reaction.